Available online at www.sciencedirect.com
ScienceDirect
Engineering Fracture Mechanics 74 (2007) 1793–1809
Engineering Fracture Mechanics
www.elsevier.com/locate/engfracmech

Numerical simulations of specimen size and mismatch effects in ductile crack growth – Part II: Near-tip stress fields

E. Østby [a,*], C. Thaulow [b], Z.L. Zhang [b]

[a] SINTEF Materials and Chemistry, N-7465, Trondheim, Norway
[b] Norwegian University of Science and Technology, N-7491, Trondheim, Norway

Received 21 September 2004; received in revised form 24 August 2006; accepted 6 September 2006
Available online 17 November 2006

Abstract

The effect of ductile crack growth on the near tip stress field in two different specimen geometries has been investigated. For homogeneous specimens it is observed that the peak stress level increases with ductile crack growth. The effect is most pronounced up to about 1 mm of crack growth. For low and intermediate hardening there is a significant effect of specimen size on the stress level. In case of mismatch in yield stress, the simulations show that the increase in stress level in the material with the lower yield stress is of a similar magnitude as is the case for stationary cracks. In case of ductile crack growth deviation from the original crack plane occurs, the highest stresses are still found close to the interface, and not in front of the current crack tip.

Keywords: Ductile crack growth; Size effect; Mismatch; Near-tip stresses; Cleavage fracture

1. Introduction

In the ductile to brittle transition region of steels, ductile crack growth often precedes the transition to cleavage fracture. Thus, the importance of ductile tearing should be included in structural assessments. Especially for thicker sections, structures may experience several millimetres of ductile crack growth before the limit capacity is reached. Also in situations where maximum utility of thinner material is sought, e.g. in the reeling of pipelines, the possibility of transition from ductile tearing to cleavage fracture should also be considered. In small scale yielding (SSY), the critical load with regard to cleavage fracture can be expressed through a critical stress intensity factor, K_{IC}, or a critical value of the J-integral, J_c. However, in most practical situations cleavage fracture will occur under conditions where there is no longer a single parameter description of the stress field at the crack tip. For such a situation, a micromechanical criterion for cleavage fracture should be included in the analysis. The use of such a criterion requires the knowledge of the stress field, and possibly other field parameters, in front of the crack tip. For stationary cracks, significant improvement

* Corresponding author. Tel.: +47 98230440; fax: +47 73592931.
E-mail address: Erling.Ostby@sintef.no (E. Østby).

0013-7944/$ - see front matter
doi:10.1016/j.engfracmech.2006.09.014

in this area has been achieved with the introduction of two-parameter fracture mechanics, where the stress field also depends on the T-stress [1] and [2] or the Q-parameter [3,4], which reflects the influence of specimen geometry and load level. For cracks in inhomogeneous material system, e.g. welds, changes in the stress field may also occur due to a difference in material properties between the different materials [5–9].

The asymptotic stress/strain fields in front of growing cracks in elastic – ideally plastic materials have been studied by Drugan et al. [10]. Their analysis revealed that the stress field in front of the growing crack bears a strong resemblance to the well-known Prandtl field found in front of stationary cracks in SSY. However, the strain field in front of a stationary crack displays a $1/r$ singularity (where r is the distance from the crack tip), while for the growing crack the strain field varies as $\ln(1/r)$. For materials displaying hardening, Dean and Hutchinson [11] and Parks et al. [12] have used FE-simulations to study the steady state fields in front of growing cracks. Although the effect of hardening modifies the nature of the fields, it is found that the stress fields for the growing cracks generally exhibits a less singular nature compared to what is found in front of stationary cracks. Varias and Shih [13] also included the effect of the T-stress on the steady state fields for growing cracks in SSY. Their analysis showed that the peak stress in front of the crack tip displayed very little dependence on the level of T-stress, indicating that a high constraint situation could prevail at the crack tip regardless of the global constraint level. Numerical simulations of crack growth in finite specimens (see e.g. [14–16]), have shown that in general the stress field will depend on the specimen geometry. However, most simulations indicate that the stress level will increase with crack growth, and increase the probability of transition to cleavage fracture. Also, the results indicate that the relative increase in stress level will be the highest for low constraint geometries. Trädegård et al. [17] argue that the Q stress could also be used in connection with growing cracks. However, because of the strong influence of the geometry no unified description of the stress field in front of growing cracks has been generally accepted so far.

In Section 3 of this paper we focus on the effect of ductile crack growth on the stress field in front of growing cracks in homogeneous specimens, i.e. no mismatch effects are included. In addition to the effect of specimen geometry, the effects of absolute specimen size and level hardening are also considered. Section 4 introduces the effect of yield stress mismatch on the stress field for interface cracks, and also discusses the main effects on the stress field in the case of crack growth deviation away from the interface.

2. Numerical procedures

The same geometries and numerical models that were used in Part I [18] of the paper are also applied in Part II. Only a brief summary of the main parameters and definitions will be presented.

2.1. Specimen geometries

Two different finite geometries are studied. The first is a shallow notched, $a/W = 0.15$, specimen loaded in predominantly tension by prescribing a uniform displacement at the ends. The second specimen geometry is a deep cracked, $a/W = 0.5$, specimen loaded in bending. The two geometries with definition of relevant dimensions are presented in Fig. 1. In the case of mismatch Mat 1 and Mat 2, Fig. 1, are modelled with different yield stress. Four different specimen sizes, $W = 25$, 50, 100, and 200 mm, are used. In the text W will be used when referring to the specimen size.

2.2. Materials

Referring to Fig. 1, the mismatch ratio between Mat 1 and Mat 2 will be defined as

$$m = \frac{\sigma_{0,2}}{\sigma_{0,1}} \tag{1}$$

where $\sigma_{0,1}$ and $\sigma_{0,2}$ are the yield stress of Mat 1 and Mat 2, respectively. The crack growth is assumed to take place in Mat 1, and this part of the specimen is modelled using a Gurson–Tvergaard–Needleman (GTN) constitutive material description. Mat 2 is modelled as a classical Mises material. The relation between plastic strain and flow stress used for Mat 2 and Mat 1 is in the form:

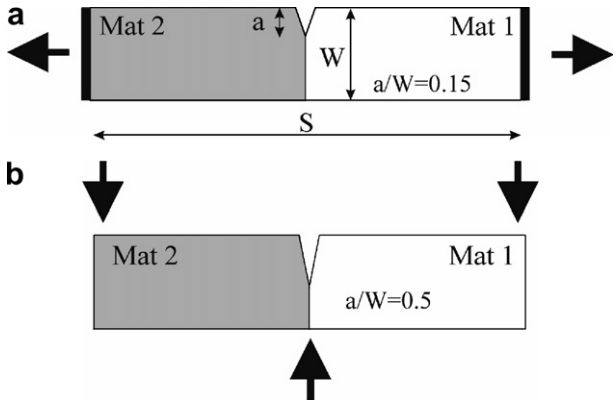

Fig. 1. The two finite geometries used in the present study. (a) Shallow cracked specimen, $a/W = 0.15$, loaded in tension. (b) Deep cracked specimen, $a/W = 0.5$, loaded in bending.

$$\bar{\sigma} = \sigma_0 \left(1 + \frac{\varepsilon_p}{\varepsilon_0}\right)^n \tag{2}$$

where $\bar{\sigma}$ is the flow stress, σ_0 is the yield stress, ε_p is the equivalent plastic strain, $\varepsilon_0 = \sigma_0/E$ is the strain at yield, and n is the hardening exponent. A fixed ratio of $E/\sigma_0 = 500$ and $\sigma_0 = 400$ is used for Mat 1 in all the analyses. The Poisson ratio is taken as $\nu = 0.3$. Further, no mismatch in elastic properties between Mat 1 and Mat 2 is assumed. The yield function of the Gurson [19] model has the following form:

$$\phi(q, \bar{\sigma}, f, \sigma_m) = \frac{q^2}{\bar{\sigma}^2} + 2q_1 f \cosh\left(\frac{3q_2\sigma_m}{2\bar{\sigma}}\right) - 1 - (q_1 f)^2 = 0 \tag{3}$$

where f is the void volume fraction, σ_m is the mean macroscopic stress, q is the conventional Mises stress, $\bar{\sigma}$ is the flow stress in the matrix material, and q_1 and q_2 are parameters introduced by Tvergaard [20,21]. Void coalescence is predicted from a modified version of Thomason's plastic limit load criterion proposed by Zhang et al. [22], further discussed in part I of this paper.

2.3. FE mesh

The FE analyses are performed using ABAQUS. Details of the near tip mesh applied can be seen in Fig. 2. The mesh consists of fully integrated 4 node elements (ABAQUS type CPE4). In the crack growth area a uniform mesh size of 0.05×0.1 mm is used. The shortest element side is parallel to the initial crack plane. Elements with an initial aspect ratio of 2 were chosen in order to reduce oscillations in the near tip stress field

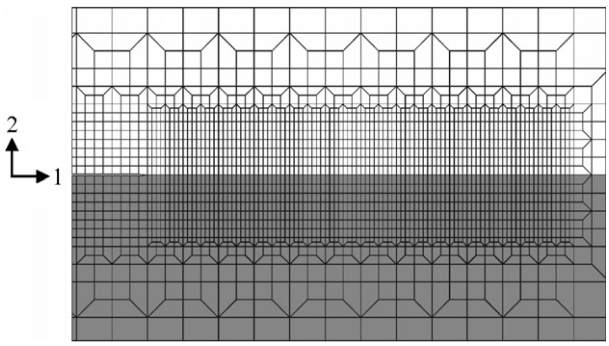

Fig. 2. Near tip details of the FE mesh used in the analyses. White area corresponds to Mat 1 and gray area corresponds to Mat 2.

in the mismatch cases, as further discussed in Part I. The extension of the area with uniform mesh size is 4.8 mm in front of the initial crack tip, and 0.7 mm in each direction normal to the interface.

3. Near tip stress distribution for growing cracks in homogeneous material

3.1. Effect of specimen geometry and size

In this section we are discussing the near tip stress and deformation fields for growing cracks in finite homogeneous specimens, i.e. no mismatch effects are included. The two specimen geometries presented in Section 2 are used in the study. In addition to the effect of specimen geometry, the effects of absolute specimen size and hardening level are also considered. Four different specimen sizes, $W = 25$, 50, 100, and 200 mm, are used, together with three different levels of hardening, $n = 0.05$, 0.1, and 0.2. Fig. 3 compares the near tip opening stress, σ_{22}, at different amounts of crack growth for various specimen sizes. For growing cracks the far-field J does not scale the stress field in the same way as for stationary cracks. Thus, the stress fields cannot easily be normalised. However, the $J-\Delta a$ curves are only slightly dependent on the specimen size, hence, the same Δa approximately corresponds to the same J for the different specimens. Fig. 3a–c show the results for the tensile specimens, $a/W = 0.15$, for the three different hardening levels, whereas the results for the bend specimens, $a/W = 0.5$, are shown in Fig. 3d–f.

For the tensile specimen with hardening $n = 0.05$, Fig. 3a, there is a clear effect of specimen size on the stress level ahead of the crack tip. The shape of the stress distribution is almost parallel for all specimen sizes, however, with some deviation for the smaller specimen, especially at large amounts of crack growth. For a given specimen size the peak stress increases slightly with crack growth. The difference in peak stress level between the largest, $W = 200$ mm, and the smallest, $W = 25$ mm, specimen is about $0.25\sigma_0$, and this difference remains virtually constant with crack growth. The results for the bending specimen with the same hardening, Fig. 3d, show that at the small amounts of crack growth there is a significant effect of specimen size on the stress level. The principal part of the void growth will take place in the unloading zone behind the peak stress. Here we will refer to the distance between the peak stress and the current crack tip as the process zone length for ductile fracture. From this definition it can be seen that the process zone length is significantly longer for larger specimen sizes in Fig. 3d. As expected, the higher influence of the global bending field for smaller specimen sizes results in a steeper gradient of the stress distribution ahead of the peak stress. With further crack growth the process zone length becomes more similar for all specimen sizes. Also, the size effect on the peak stress is reduced, and remains almost constant with further crack growth. The influence of specimen size on the slope of the stress distribution is still significant. Again, for a given specimen size the stress level increases slightly with crack growth. We note one special case for the largest specimen size, $W = 200$, at 1 mm of crack growth, Fig. 3d, where the stress distribution displays two "peaks". Comparing the results of the tensile and bend specimens for this hardening level, one finds that the difference in the peak stress, when compared for the same W (this comparison is a mere formal choice), is about $0.5\sigma_0$, which indicates a strong effect of geometry constraint also in the case of growing cracks. The process zone length is about twice as large in the bending specimen compared to that in the tensile specimen, which is in line with the observations of Xia and Shih [23] from modified boundary layer (MBL) studies on the effect of T-stress on the process zone length. However, both the size effect on the peak stress, and the increase in the peak stress with crack growth for a given specimen size, are about the same for both specimen geometries. The results for the tensile specimen with hardening $n = 0.1$ can be seen in Fig. 3b. The trends are similar to the tensile specimens with hardening $n = 0.05$, Fig. 3a. Comparing the bend specimen with hardening $n = 0.1$, Fig 3e, with the results for $n = 0.05$, it is clear that the trends are also very similar for this geometry. A slight increase in peak stress with crack growth is noted for all specimen sizes. The size effect on the peak stress is slightly lower compared to the hardening level $n = 0.05$. When comparing the peak stress between the tensile and bend specimen for the hardening level $n = 0.1$ for the same W, it is found that this difference is about 0.3–$0.35\sigma_0$, with the largest difference for the smallest W. Thus, the effect of specimen geometry on the peak stress level is reduced compared to the hardening level $n = 0.05$. The results for the highest hardening level, $n = 0.2$, display stronger differences compared to the two lower hardening levels. From the results for the tensile specimens, Fig. 3c, it is seen that the specimen size has virtually no effect on the peak stress. However, the slope of the stress distribution is steeper for smaller specimen sizes. Roughly the

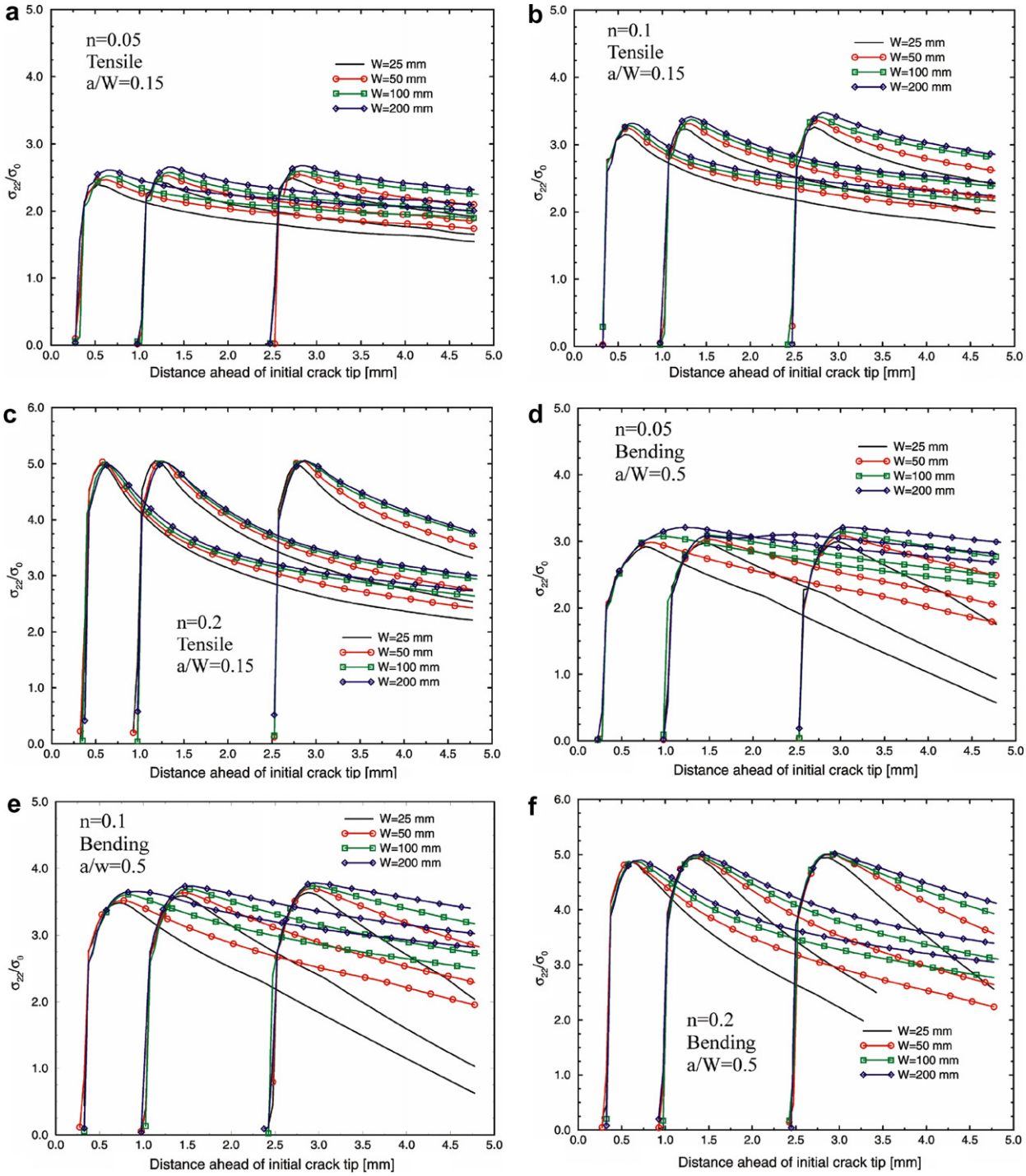

Fig. 3. Effects of crack growth and specimen size on opening stress distribution ahead of the current crack tip. (a–c) Tensile specimens, $a/W = 0.15$. (d–f) Bending specimens, $a/W = 0.5$. (a) and (d) $n = 0.05$. (b) and (e) $n = 0.1$. (c) and (f) $n = 0.2$.

same trends are also observed for the bending specimen with $n = 0.2$, Fig. 3f. There is a less distinct effect of the specimen size on the peak stress, except for the smallest specimen, $W = 25$ mm, but the different influence of the global bending field on the slope of the stress distribution is still clearly evident. When comparing the

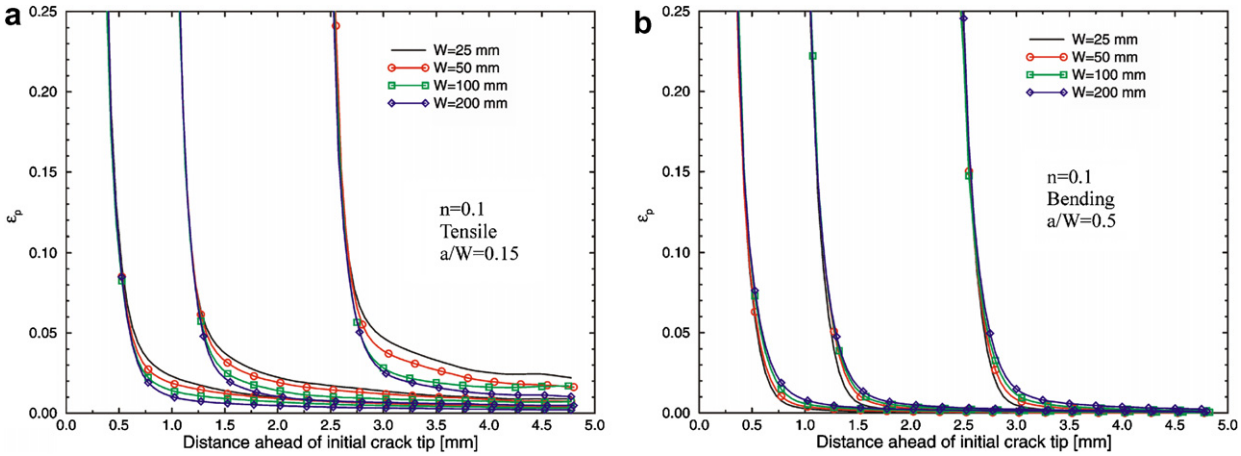

Fig. 4. Effects of crack growth and specimen size on plastic strain distribution ahead of the current crack tip for hardening $n = 0.1$. (a) Tensile specimens, $a/W = 0.15$. (b) Bending specimens, $a/W = 0.5$.

results for the tensile and bend specimen for the hardening level $n = 0.2$, it is noted that the peak stress level is more or less the same for both specimen types.

The discussion above has focused on the effect of specimen size on the distribution of the opening stress for growing cracks. Some important effects of specimen size can also be observed for the distribution of plastic strain ahead of the crack tip, here the selected results are shown for the case with $n = 0.1$. Fig. 4a and b show the influence of specimen size on the plastic strain distribution for the tensile and bending specimens, respectively, with different amounts of crack growth. For the tensile specimen it is seen that the plastic strain ahead of the intense deformation in the process zone, increases with decreasing specimen size. Also, the plastic strain level increases with crack growth, due to the increasing deformation in the remaining ligament. For the bending specimen the opposite trend with regard to the effect of specimen size is observed, and the plastic strain level decreases with decreasing specimen size. This is due to the different influence of the global deformation field on the near tip conditions in the two geometries. In the tensile specimens the principal global deformation in a 45° direction to the ligament strongly interacts with the near tip deformation field. Further, for a given amount of crack growth the deformation will be higher in the smaller specimens resulting in a higher plastic strain level. In the bend specimens the steeper gradient in the bending field for smaller specimen sizes causes a slightly decreasing plastic strain level ahead of the process zone for decreasing specimen size. As expected, the plastic strain level is significantly higher in the tensile specimen compared to the bend specimen. Similar results also exist for the other hardening levels.

In the literature the J value at the initiation of ductile crack growth does not display a very strong dependence on specimen geometry [24], which is also supported by results from numerical simulations [25]. This result also applies with regard to the effect of specimen size, with a possible exception for tensile specimen with high hardening, as seen from numerical simulation of the $J - \Delta a$ curves in Fig. 4 in Part I of this paper. However, for equal J values the deformation level in the specimens will depend on the size W. This can be seen in Fig. 5, which compares the normalised load per unit thickness and the crack growth vs. the normalised global displacement for the tensile and bending specimens respectively. The results are for hardening $n = 0.1$. For the smallest specimen size, $W = 25$ mm, crack growth is initiated after significant global plasticity has developed in the specimen. In contrast, for the largest specimen size, $W = 200$ mm, only a small deviation from the initial linear slope of the load displacement curve is observed at initiation. Fully plastic analyses of constraint in finite specimens show that the Q-stress will be reduced with increasing global deformation. Thus, the constraint level at the initiation of ductile crack growth will decrease with decreasing specimen size, and the stress level should initially be lower in the smaller specimens as seen from Fig. 3.

Fig. 6 shows the history of the peak stress with crack growth. In tensile specimens, Fig. 6a, it can be seen that the increase in peak stress is somewhat higher for small amounts of crack growth, up to 0.5–1 mm. An exception is seen for the largest specimen, $W = 200$ mm, with $n = 0.05$. Here the effect of loss of constraint due

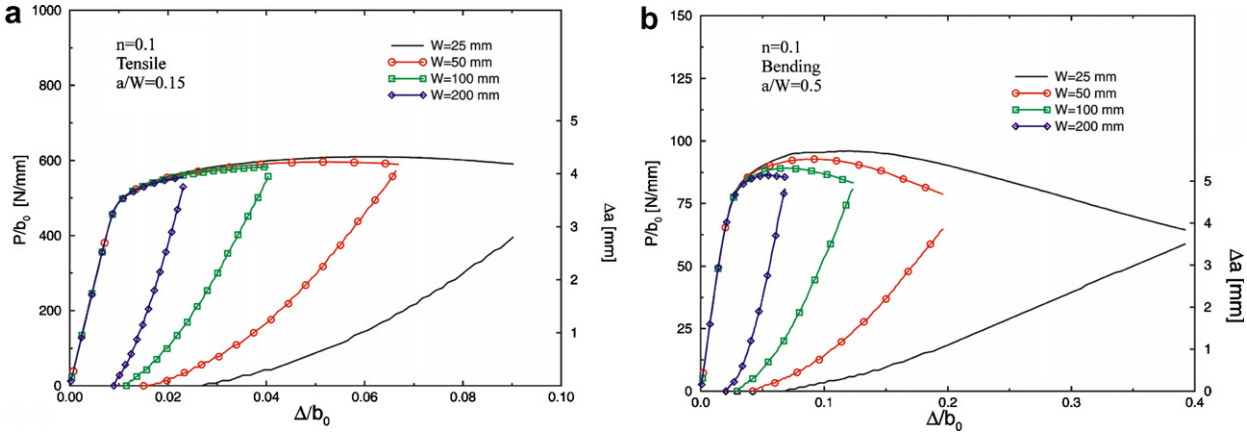

Fig. 5. Comparison between (a) load vs. displacement, tensile specimens, $a/W = 0.15$, both axis normalized with initial ligament b_0, and (b) ductile crack growth vs. displacement, bending specimens, $a/W = 0.5$, normalized with b_0.

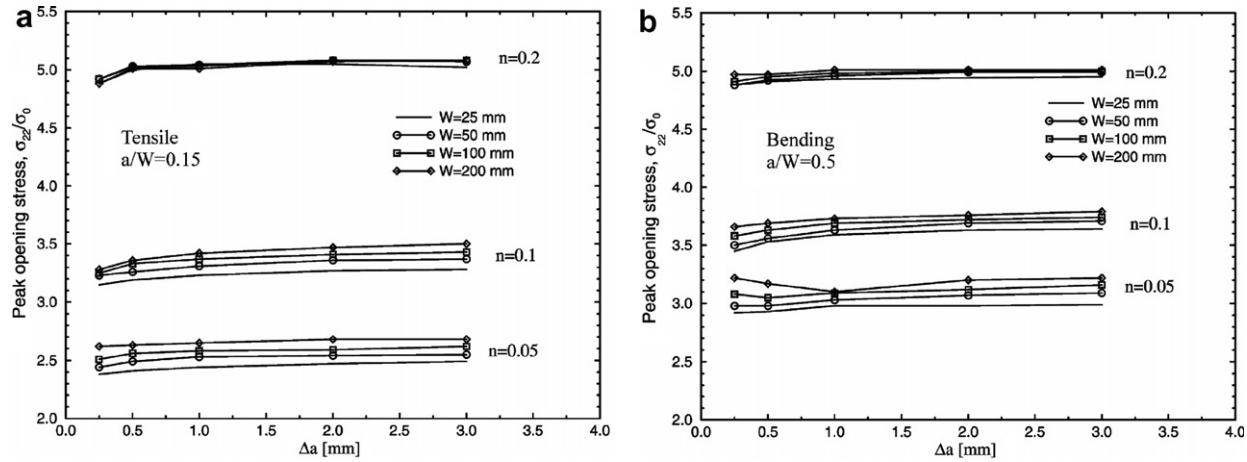

Fig. 6. Comparison of evolution of peak opening stress with crack growth for the different specimen sizes and hardening levels. (a) Tensile specimens, $a/W = 0.15$. (b) Bending specimens, $a/W = 0.5$.

to increase in global deformation is higher than the effect of crack growth, and a decrease in peak stress is seen for small amounts of crack growth. At larger amounts of crack growth, 1 mm and more, a more unified picture emerges. In this zone, a weaker increase in stress level with crack growth is observed. The reason for the initially higher increase in the stress level is further discussed in Section 3.3. For the hardening levels $n = 0.05$ and 0.1 a significant effect of specimen size on the peak stress level can also be seen. Further, this effect remains almost constant with crack growth. For the high hardening case, $n = 0.2$, the size effect on the peak stress is negligible, in accordance with Fig. 3c. In the bending specimens, Fig. 6b, the behaviour is less uniform for small amounts of crack growth. For low hardening, $n = 0.05$, a decrease in the peak stress is actually seen initially, being most prominent in larger specimen sizes. This effect is similar, but more significant compared to what was observed for the largest tensile specimen with the same hardening in Fig. 6a. A possible reason for the stronger effect in the bend specimens could be the larger process zone. This results in the local effect of crack growth being "felt" less strongly at the location of the peak stress, and the effect of loss of constraint due to an increased global deformation will dominate the peak stress level at the small amounts of crack growth. However, for both $n = 0.1$ and 0.2 an increase in stress level is observed initially, as for the tensile specimens. For the larger amounts of crack growth, the behaviour is similar to the tensile specimens, with

a weak increase in stress level with crack growth. Also, the size effect on the stress level for $n = 0.05$ and 0.1 remains mostly constant with crack growth and is of almost equal magnitude as for the tensile specimens. Again, it can be seen that the size effect on the peak stress is significantly smaller for the high hardening. The main observation from the above results is that in general the size effect on the peak stress level remains almost constant with crack growth, and is mainly given by the difference in constraint level at initiation.

3.2. Effect of initial void volume fraction

In the presentation of the results above we have assumed a fixed value $f_0 = 0.002$ for the initial void volume fraction. Here we seek to gain some insight in the effect of the ductility of the material on the stress distribution ahead of the growing crack by applying different values of f_0. We compare three different values of $f_0 = 0.0005$, 0.002, and 0.005. Further, a fixed specimen size, $W = 50$ mm, with hardening level $n = 0.1$, is used in the discussion. In Fig. 7, the effect of f_0 on the opening stress for different amounts of crack growth is shown, both for a case with a tensile specimen Fig. 7a, and a bending specimen, Fig. 7b. Three main observations are made from these figures:

- First, the stress level increases with decreasing f_0.
- Second, for small amounts of crack growth, there is a significant difference in process zone length, with an increasing length for decreasing f_0. This is further discussed in Section 3.3.
- Third, for the crack growth about 1 mm and more, the shape of the stress distribution is similar for all values of f_0.

With regard to the first observation, Xia and Shih [23] pointed out that the stress level was mainly given by the choice of f_0. From Fig. 7, it can be seen that for 1 mm or more of ductile tearing, the stress fields are more or less shifted vertically with a constant factor when f_0 is changed. As f_0 is decreasing, the ductility of the material increases and more deformation is needed to reach a certain amount of crack growth. The global deformation required is linked to the global load in the specimen. The reduction in stress level is 4–5% and 8–9% for the cases with $f_0 = 0.002$ and 0.005, respectively, compared to the case with $f_0 = 0.0005$. This corresponds well with the reductions in the global load level, which are 4.5% and 9%, for the same cases when compared with the $f_0 = 0.0005$ case for the same amount of ductile tearing. Thus, this indicates that the difference in stress level observed with changing f_0 of the material is mainly reflecting the higher global load observed in specimens with decreasing f_0.

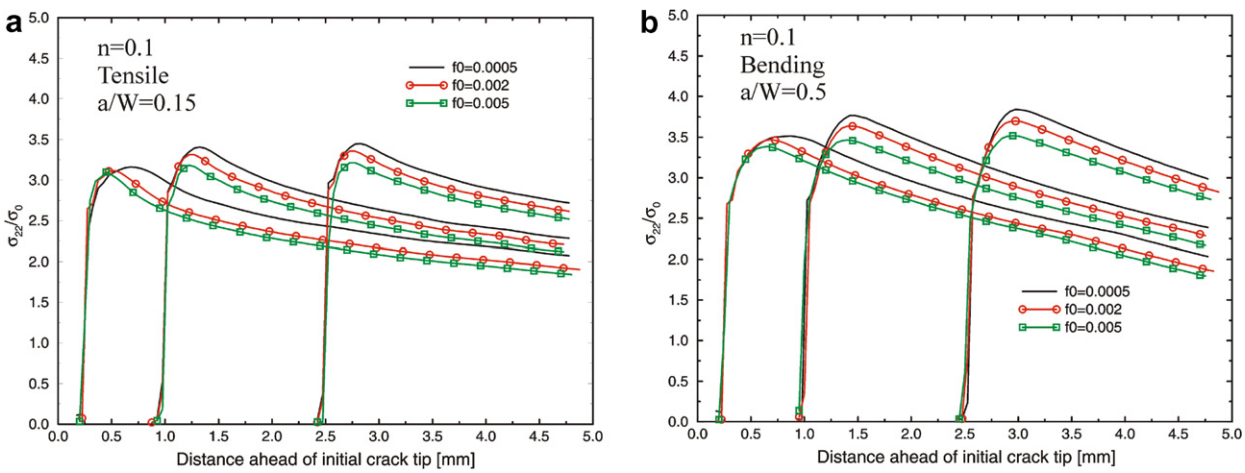

Fig. 7. Effect of varying initial void volume fraction, f_0, on the opening stress distribution for different amounts of crack growth. Specimen size $W = 50$ mm and hardening $n = 0.1$. (a) Tensile specimen, $a/W = 0.15$. (b) Bending specimen, $a/W = 0.5$.

3.3. Crack tip deformation for small amounts of crack growth

In Figs. 6 and 7, there is a tendency for the peak stress to increase most for the small amounts of ductile crack growth. In Fig. 8, the history of local fracture strain in front of the current crack tip as a function of ductile crack growth is shown for the different levels of f_0. The results are for hardening $n = 0.1$ and specimen size $W = 50$ mm. For the tensile specimens Fig. 8a, it can be seen that for the small amounts of crack growth a reduction in fracture strain is observed with crack growth. Due to this the opening at the current crack tip will be reduced or become sharper. This geometry change will influence the stress level close to the crack tip. The effect of this will contribute to the initially higher increase in the peak stress that is seen for the small amounts of ductile crack growth in Fig. 6a. From Fig. 8a it can also be seen that the drop in fracture strain with crack growth is more significant for the lower values of f_0, and the change in local crack tip geometry will be more significant. This corresponds to the observation in Fig. 7a, where a higher initial increase in the stress level is observed for the case with $f_0 = 0.0005$ compared to the case with $f_0 = 0.005$. For the larger amounts of crack growth, the fracture strain changes very little, and the local crack tip geometry remains virtually constant. In this region only a slight increase in the stress level is observed due to an increase in the ligament load, as seen in Fig. 6a. The fracture strain history for the bending specimens with different f_0 is shown in Fig. 8b. In principle the same behaviour is seen as for the tensile specimens, with decreasing fracture strain up to about 1 mm. The effect is most significant for the lowest f_0. However, for the very small amounts of crack growth the behaviour differs from the tensile specimens, and a small increase in fracture strain is observed up to about 0.25 mm of crack growth for the two highest f_0 levels. For the larger amounts of crack growth, the fracture strain remains virtually constant as for the tensile specimens.

3.4. Main features of the stress fields

In principle the evolution of the near tip stress field may be divided into three phases:

1. Blunting phase.
2. Transition from blunting to growth-controlled phase.
3. Growth phase.

The blunting-controlled phase is not discussed in this paper. The transition from the blunting to the growth-controlled phase is characterised by geometrical changes in the local crack tip geometry as the crack grows out of the blunting-dominated zone. A reduction in the local fracture strain with crack growth is

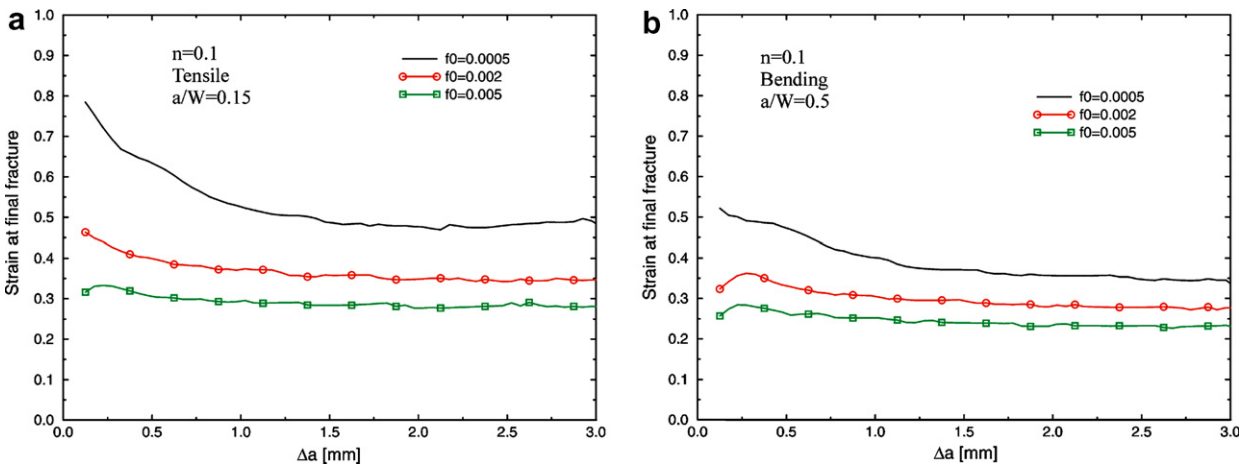

Fig. 8. History of local fracture strain with crack growth for different assumptions of initial void volume fraction, f_0. Specimen size $W = 50$ mm and hardening $n = 0.1$. (a) Tensile specimen, $a/W = 0.15$. (b) Bending specimen, $a/W = 0.5$.

observed, decreasing the local crack tip opening. This sharpening of the local crack tip, together with the increase in the global load, will result in an increased peak stress compared to what is observed for the larger amounts of crack growth. The influence of the transition zone is larger for materials with a higher ductility, which experiences more blunting before the initiation of ductile crack growth. The length of the transition zone cannot be sharply defined, and in general, it depends on the material properties. However, the main influence of this zone can be found up to 0.5–1 mm of the crack growth.

After roughly 1 mm of crack growth, only a very small change in local fracture strain with further crack growth is observed. Here the process zone length remains more or less constant, and the deformation necessary to sustain ductile crack growth is fed from the intense plastic deformation field moving through the ligament with the growth of the crack. The peak stress increases slightly with crack growth due to the increase in the ligament load. For the shallow notched tensile specimens the effect of specimen size on the peak stress remains almost constant with crack growth in this zone for low and intermediate hardening. Further, near the crack tip the stress fields for different specimen sizes are nearly parallel.

4. Effect of mismatch on stress field for growing cracks

In Section 3 the effect of ductile crack growth on the near tip stress distribution in a homogeneous material was investigated. In steel structures, the most brittle microstructures are often found in relation to weldments. Especially cracks located close to the fusion line tend to display a brittle behaviour. This is partly due to the thermal cycles from the welding process changing the microstructure, leaving it more brittle. However, a second reason for the more brittle behaviour can also the change in the stress field due to an additional constraint from the surrounding materials with different plastic properties (yield stress/hardening). The situation with the fusion line crack can be studied in an idealised way by assuming a crack to lie on the interface between two different materials. Such models have received a considerable attention in the literature for stationary cracks (see e.g. [5–9]). The main findings from these studies have been that the stress level in the weaker material (the material with the lowest yield stress) is increased close to the crack tip compared to what is found for the homogeneous material. For materials displaying a mismatch in the yield stress, Zhang et al. [6] found that the stress fields in a small scale yielding could be closely approximated by introducing an additional term, representing the difference field due to mismatch, depending on the yield stress mismatch, m, between the two materials. Østby et al. [26] studied the same situation in the case of materials displaying a mismatch in hardening, and found that the change in the near tip stress field was mainly characterised by the difference in hardening exponent, termed Δn, between the two materials. Few results have been reported for the effect of mismatch in case of ductile crack growth. Moran and Shih [27] and Burstow and Howard [28] considered the effect of mismatch for cracks located in the centre of weldments, and thus not specially considered the interface problem. Hao et al. [29] simulated crack growth in mismatched specimens with interface cracks, but did not focus on the stress field with regard to cleavage fracture. Here we concentrate on the effect of mismatch on the stress level ahead of the growing crack. In Section 4.1 we consider the case where the crack is "forced" to grow along the interface. However, an additional feature due to the possible deviation of the crack growth away from the interface arises for the interface cracks, and the principal effects of this on the stress field are discussed in Section 4.2.

4.1. Ductile crack growth along the interface

The ductile crack growth along the interface between the two materials is studied by only using a Gurson constitutive description in the first layer of elements in Mat 1. Ductile crack growth is then only allowed to take place in Mat 1 along the interface. Three levels of yield stress mismatch, $m = 1.125$, 1.25, and 1.5, are examined, with a fixed specimen size of $W = 50$ mm and $f_0 = 0.002$. The hardening exponent, n, is equal in both Mat 1 and 2. Fig. 9 shows the effect of mismatch on different stress components and equivalent plastic strain in Mat 1 for the layer of elements along the interface, for the tensile case with $n = 0.1$. From Fig. 9a it can be seen that mismatch does not have a very strong effect on the opening stress, σ_{22}, normal to the interface, and only a slight elevation compared to $m = 1$ is observed. Further, the small elevation does not depend on the level of mismatch. A much stronger effect of mismatch is seen for the stress component parallel to the inter-

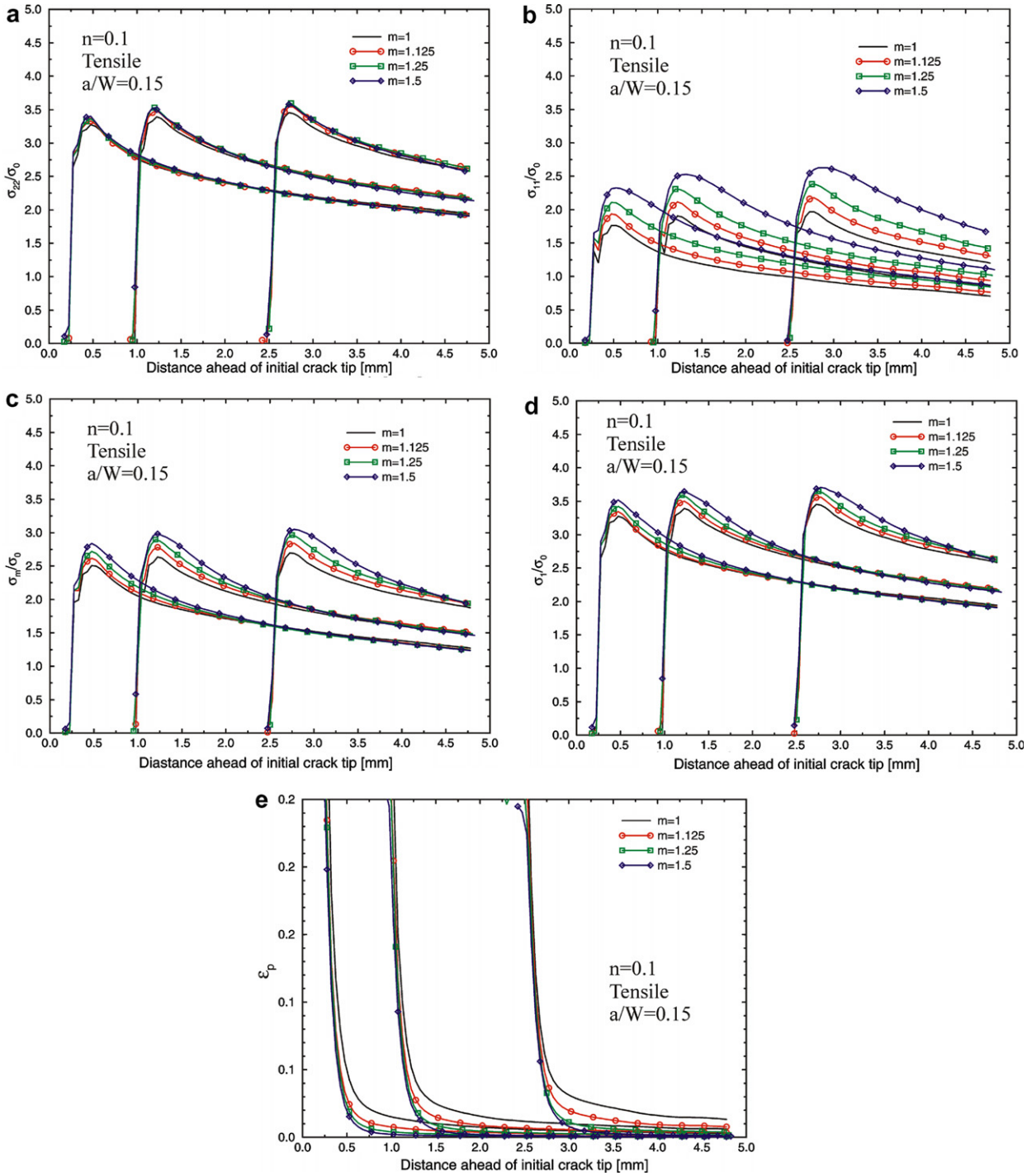

Fig. 9. Effect of mismatch and crack growth on the distribution of different stress components and plastic strain ahead of the current crack tip. Tensile specimen, $a/W = 0.15$, $W = 50$ mm and $n = 0.1$. (a) Opening stress, σ_{22}. (b) Stress parallel to interface, σ_{11}. (c) Hydrostatic stress, σ_m. (d) First principal stress, σ_1. (e) Equivalent plastic strain, ε_p.

face, σ_{11}, in Fig. 9b. It is also observed that the increase in σ_{11} is strongly dependent on the level of mismatch, and close to the crack tip the increase is about $0.6\sigma_0$ for the case with $m = 1.5$ compared to $m = 1$. The increase due to mismatch of the hydrostatic stress component, σ_m Fig. 9c, is between σ_{11} and σ_{22}. Due

to the introduction of shear stresses along the interface the principal stress, σ_1, will not be parallel to the opening stress, and an increase due to mismatch is also observed for this stress component as seen in Fig. 9d. A slight increase in the difference in principal stress can be observed with crack growth from this figure. The equivalent plastic strain ahead of the intense deformation zone is also influenced by the mismatch constraint, giving a lower plastic strain for the increasing mismatch Fig. 9e.

The effects discussed above will also depend on the hardening level and the specimen geometry. Here we are considering the effect of these parameters on the principal stress along the interface for the three levels of n and the two specimen geometries. The same mismatch levels, specimen size, $W = 50$ mm, and $f_0 = 0.002$, as described above are used. Due to the tendency for the analyses to become unstable, especially in the case of high mismatch levels for the bending specimens and for the high levels of hardening in general, the results are not complete. However, some main conclusion can still be drawn based on the results presented.

The results for the tensile specimen for the hardening levels $n = 0.05$, 0.1, and 0.2 can be seen in Fig. 10a–c, respectively. The increase in principal stress is highest for the lowest hardening level, and the effect decreases with higher hardening. Especially, for $n = 0.2$, virtually no effect of mismatch can be seen in the principal stress level, apart from some differences in the peak stress for very small amounts of crack growth. It is also noted that the effect of "saturation" of the principal stress level for a high mismatch, $m = 1.5$, close to the crack tip is stronger for the lowest hardening, $n = 0.05$ Fig. 10a, than for the case with $n = 0.1$, Fig. 10b. Thus, the effect of non-proportional loading close to the crack tip for high mismatch levels increases for decreasing hardening. Fewer results are available for the bending specimen, Fig. 10d–f, because of the tendency for the analysis to become unstable. However, much the same behaviour as observed for the tensile specimen is also evident for this specimen geometry. The relative effect of increase in principal stress level due to mismatch is highest for the lowest hardening, $n = 0.05$ Fig. 10d, while almost no effect is observed after some crack growth for the highest hardening level, $n = 0.2$ Fig. 10f. A comparison between the tensile and bending specimens indicates a higher increase in the stress level due to mismatch for the latter geometry, with a more pronounced increase in the peak principal stress level for the same level of mismatch.

For mismatch in the case of stationary interface cracks in SSY, Zhang et al. [6] report an increase in the principal stress level close to the crack tip of about $0.35\sigma_0$ and $0.6\sigma_0$ compared to the situation with $m = 1$, for the cases with $m = 1.25$ and 1.5, respectively, for a material with hardening $n = 0.1$. For the tensile specimen with the same hardening, Fig. 10b, it is seen that the increase in peak stress due to mismatch at 1 mm of crack growth is about $0.2\sigma_0$ and $0.3\sigma_0$, for the same mismatch levels. Thus, the observed increase in the principal stress is lower for the tensile specimen with ductile crack growth compared to the SSY solution for stationary cracks. However, the lower effect of mismatch for the tensile specimen is consistent with results reported by Thaulow et al. [30] for tensile specimens with stationary cracks. For the bending specimen Fig. 10e, the increase in the peak stress at 1 mm of crack growth for the case with $m = 1.25$ is about $0.3\sigma_0$. As mentioned above, the analysis did not converge for the case with $m = 1.5$ for $f_0 = 0.002$. However, the results obtained with $f_0 = 0.0005$ gave an increase in the peak stress of about $0.5\sigma_0$ at 1 mm of crack growth for the case with $m = 1.5$. From this the increase in the principal stress due to mismatch for the bending specimens is similar to what is found for the stationary cracks in SSY. These results indicate that for the hardening level $n = 0.1$ the effect of mismatch in the case of the ductile crack growth is of a similar magnitude to the effect of mismatch found for stationary cracks with the same mismatch levels. For high hardening, $n = 0.2$, the effect of mismatch in the case of ductile crack growth differs from the same results for stationary cracks. Zhang et al. [6] report a similar increase in the principal stress for the case with $n = 0.2$ as for $n = 0.1$ for stationary cracks in SSY. From Fig. 10c and f, as pointed out above, it is seen that virtually no increase in principal stress with mismatch is observed for crack growth of 1 mm or more, for both the tensile and the bending specimen. However, at a small amount of crack growth an effect of mismatch on the peak principal stress can still be seen, but this effect diminishes very rapidly with crack growth. Further, a slightly more pronounced effect of the mismatch is seen for the hydrostatic stress level close to the crack-tip. Some analyses were also run with mismatch in the hardening exponent, n, between Mat 1 and Mat 2. These results are not presented in detail here, but the results showed that an increase in the near tip stress level was also observed in the material with the lowest hardening as seen in the case of stationary cracks. However, the relative effect of difference in hardening mismatch level tends to be somewhat smaller compared to that reported for stationary cracks in SSY by Østby et al. [26], especially for the tensile specimens.

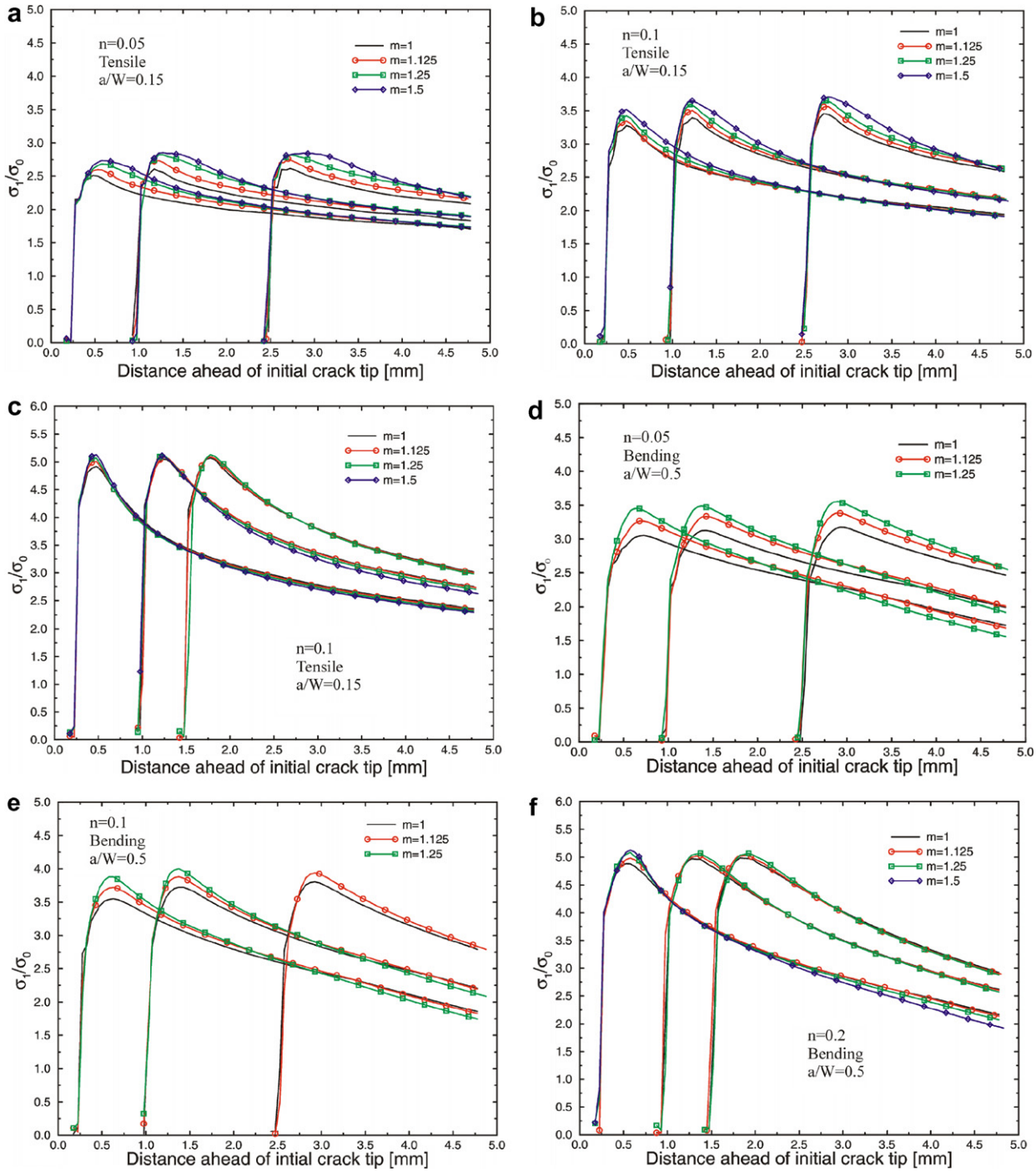

Fig. 10. Effect of mismatch on the principal stress distribution for different hardening levels and specimen geometries. (a–c) Tensile specimens, $a/W = 0.15$. (d–f) Bending specimens, $a/W = 0.5$. (a) and (d) $n = 0.05$. (b) and (e) $n = 0.1$. (c) and (f) $n = 0.2$.

4.2. The effect of crack growth deviation

Experience has shown that the ductile crack growth for cracks initially located close to the fusion line in weldments with mismatch often tends to deviate away from the original crack plane Thaulow et al. [9]. The

crack growth is shifted into the material with the lower yield stress where the plastic deformation is focused. In Part I of this paper, numerical simulations were used to study the ductile crack growth in bi-material specimens with mismatch in the yield stress for cracks initially lying on the interface between the two materials. The results from these simulations indicate that the growth direction is mainly influenced by two factors: the hardening in the material in which the growth is assumed to take place and the mode of loading. The tendency for crack growth deviation was found to increase for materials exhibiting a low strain hardening. Further, the influence of a strong global bending deformation seemed to promote a stronger deviation than tensile loading. Some influence from the level of mismatch was also found, but this was less significant than the two factors mentioned above. With regard to the cleavage fracture, it is of great interest to establish an understanding of the effect of such a deviation on the stress field close to the crack tip. However, the deviation introduces some features making a simple field description more difficult. Because the distance between the current

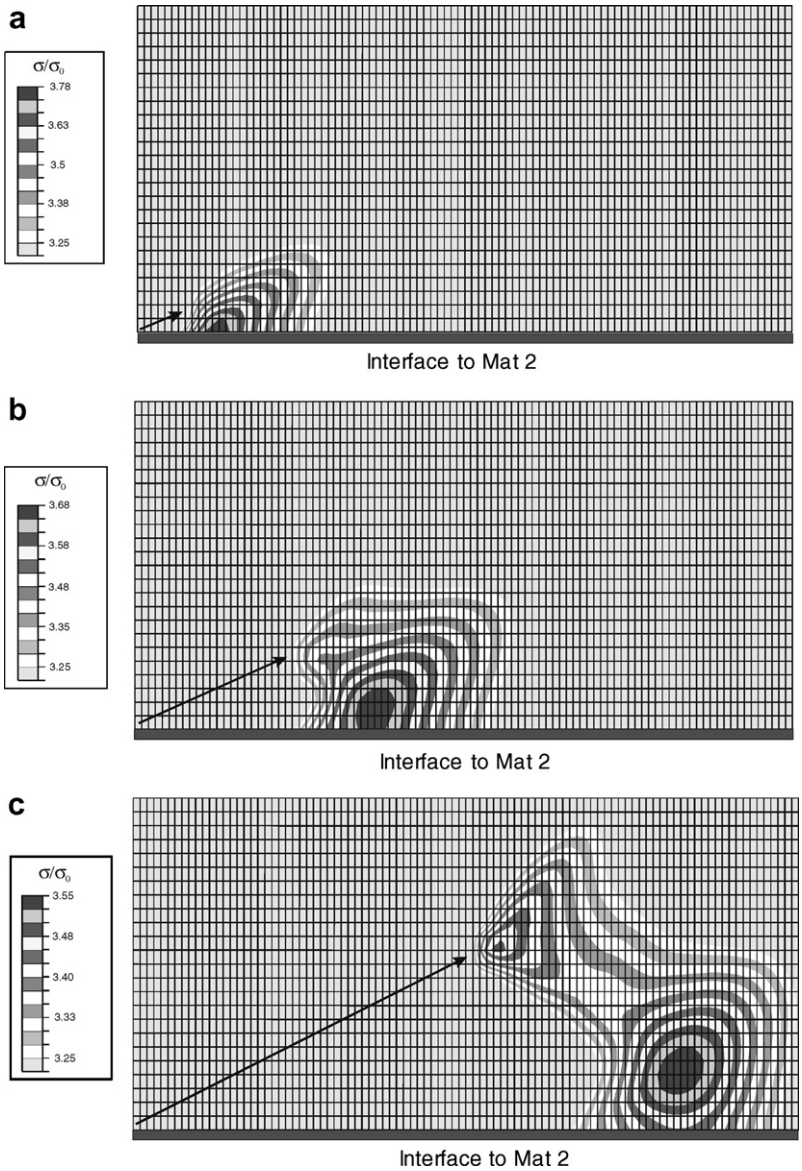

Fig. 11. Effect of crack growth deviation on principal stress distribution. Bending specimen, $a/W = 0.5$, $W = 50$ mm, mismatch level $m = 1.25$, and hardening $n = 0.1$. The black arrow indicates the principal crack growth path, with the tip of the arrow pointing at the current crack tip. (a) Crack growth about 0.3 mm. (b) Crack growth about 1 mm. (c) Crack growth about 2.5 mm.

crack tip and the interface is changing, a non-constant length scale will be introduced into the problem. We will now discuss the main features related to the deviation of ductile crack growth by means of an example. The example consists of a bending specimen with hardening $n = 0.1$ and mismatch level $m = 1.25$, with crack deviation occurring at about 30° to the interface into Mat 1. Comparisons for the same case with "forced" crack growth along the interface are also made.

Fig. 11 shows contour plots of the principal stress distribution at the different stages of crack growth/deviation. In Fig. 11a the crack has grown about 0.35 mm along the interface, and the current crack tip has shifted to the second layer of elements. It can be seen that the highest principal stress, $3.78\sigma_0$, is not at the crack tip but appears at the interface between the two materials. After further crack deviation, Fig. 11b, it can be seen that two stress peaks develop. The highest peak stress, and the largest area of high stress, however, is still at the interface. The value of the highest principal stress is reduced to about $3.68\sigma_0$. In the last figure, Fig. 11c, the current crack tip has moved about 1.2 mm away from the interface. In this figure the two peaks are even more distinct. The highest principal stress still occurs in the vicinity of the interface, but has now moved somewhat into the material. The value of the peak principal stress has decreased to $3.55\sigma_0$. By comparison with the case $m = 1.25$ in Fig. 10e, showing the results for the "forced" crack growth along the interface, the peak principal stress for about the same amounts of crack growth are about $3.8\sigma_0$, $4.0\sigma_0$, and $4.1\sigma_0$ (the latter value is extrapolated). Thus, it is seen that while the peak stress increases with crack growth when the crack grows along the interface, the opposite is the case for deviating cracks. For about 2.5 mm of crack growth along the interface, the difference in peak stress between the two cases is about $0.55\sigma_0$. The peak stress in front of the current crack tip remains constant at about 3.5–$3.55\sigma_0$ with crack growth. This is also lower than for the homogeneous case with $m = 1$ and straight crack growth in Fig. 10e, where the peak stress level starts at about $3.55\sigma_0$ and increases to about $3.8\sigma_0$ after 2.5 mm of crack growth.

As mentioned above, the numerical simulations indicate that the degree of crack growth deviation will depend on both hardening level and mode of loading. From Fig. 6 in Part I [18] of this paper it can be seen that for hardening $n = 0.05$ a strong crack growth deviation is observed for both the tensile and bend specimens in case of mismatch. In these specimens a reduction in the peak principal stress level is also observed as the current crack tip moves away from the interface. After the crack has deviated about 1 mm from the interface, the reduction in the peak principal stress level is about $0.45\sigma_0$ and $0.55\sigma_0$, respectively, compared to the analyses with growth along the interface in Fig. 10a and d, for the case with $m = 1.25$. These reductions are similar to the observed reduction in the principal stress in the example above. For the tensile specimens with $n = 0.1$, Fig. 10b, in Part I, the tendency to deviation is negligible, and the stress level is similar in the case of growth along the interface and weak deviation. Thus, the reduction in the peak stress is closely related to the amount of deviation from the interface.

From a peak stress point of view, the crack growth deviation should have a beneficial effect on a possible initiation of cleavage fracture, both with regard to the stress level close to the interface and at the current crack tip. However, even though crack deviation occurs, the highest stresses still appear close to the interface. This sampling effect is probably of importance for the highly non-homogeneous microstructure found at the fusion line in steel weldments. Given that the initiation of cleavage fracture is controlled by both the probability of hitting a brittle microstructure and the local stress level, some of the seemingly beneficial effect of ductile crack growth deviation may be lost due to the larger material volume sampled.

5. Summary and discussion

The numerical analyses of ductile crack growth confirm that the stress level ahead of the crack tip will increase with ductile crack growth. The increase in stress level is most pronounced for the small amounts of crack growth, up to about 1 mm. For the small amounts of ductile crack growth, a decrease in the local fracture strain with crack growth is observed. This is most clearly seen for materials with a high ductility (i.e. low initial void volume fraction), which changes the local crack tip geometry. In addition to the expected effect of specimen geometry, the numerical simulations have also revealed a significant effect from specimen size on the stress level. The size effect is due to the different constraint levels in the specimens at the initiation of ductile crack growth, and remains more or less constant with further crack growth. However, both the effects of specimen geometry and size depend rather strongly on the material hardening. For low hardening,

the effect of both specimen geometry and size are more significant. This agrees with McClintock's [31] prediction of a geometry dependent stress field ahead of the crack tip in perfectly plastic materials. When the material displays a high hardening, the hardening characteristic of the material dominates the stress level close to the crack tip, and both the geometry and size effects are strongly reduced.

For the cracks lying initially on the interface between the two materials with mismatch in the yield stress, an increase in the principal stress level is observed compared to what is found in the homogeneous material. The stress level increases with increasing mismatch, but does not display a strong dependence on the amount of ductile crack growth. However, in some cases with a high level of mismatch and a low hardening, an increasing tendency to "saturation" of the stress level with crack growth ahead of the crack tip is seen. As for the geometry and size effects in the homogeneous specimens, the relative effect of mismatch on the stress level is the highest in the case of a low hardening. For a high hardening virtually no increase in the principal stress due to mismatch is observed, once a small amount of crack growth has occurred. Comparisons with the results from the literature (Zhang et al. [6]) have revealed that for intermediate hardening levels the mismatch effect is of a comparable magnitude to that of stationary cracks. Allowance for crack growth deviation to occur reduces the detrimental effect of mismatch on the peak stress level compared to the cases where the cracks are "forced" to grow along the interface. However, it is noted that the highest stress level is still found close to the interface even when deviation occurs. This is the area where the most brittle microstructures are expected to be found in case of cracks lying close to the fusion line in steel weldments. The observation explains why the initiation of cleavage fracture is often observed close to the interface, even if ductile crack growth deviation appears before the initiation of cleavage fracture.

With regard to cleavage fracture the effect of increasing stress level should be included in fracture assessments for cases where the structure should be able to undergo a large inelastic deformation without fracturing. In order to quantify the effect of the change in the stress field the analyses above should be coupled with a micromechanical cleavage fracture criterion. The Weibull stress approach for cleavage fracture predictions (Beremin [32]) could be of valuable use in this context. The adoption of a toughness scaling approach for the use of the Weibull stress, i.e. to transfer fracture toughness between different geometries, as proposed by Xia and Shih [33] and Ruggieri and Dodds [16] could be a fruitful use of the model. For stationary cracks the constraint level can either be expressed through the T-stress or the Q-parameter, Thaulow et al. [34]. Some differences exist between the stationary fields and those found in the case of crack growth. In the stationary case the peak stress will in general decrease monotonically with increasing load, but the opposite is observed in case of ductile crack growth. Further, the extent of the zone of high stresses and the unloading zone in front of the crack tip must scale with the applied global J in order to obtain "self similarity". For the growing cracks the far field J contains a history effect from the unloaded zone behind the crack tip, and does not scale the extent of the zone of high stress as for the stationary crack. These differences pose restrictions for applying the concept of the T-stress or the Q-parameter directly to the growing cracks.

Acknowledgement

The support from the Norwegian Research Council and Statoil, together with support from the ECSC/industry sponsored research project PRESS, for this work is highly acknowledged.

References

[1] Du ZZ, Hancock JW. The effect of non-singular stresses on crack-tip constraint. J Mech Phys Solids 1991;39:555–67.
[2] Betegon C, Hancock JW. Two-parameter characterization of elastic-plastic crack-tip fields. J Appl Mech 1991;50:104–10.
[3] O'Dowd NP, Shih CF. Family of crack-tip fields characterized by a triaxiality parameter – I. Structure of fields. J Mech Phys Solids 1991;39:989–1015.
[4] O'Dowd NP, Shih CF. Family of crack-tip fields characterized by a triaxiality parameter – II Fracture application. J Mech Phys Solids 1992;40:939–63.
[5] Shih CF, Asaro RJ. Elastic–plastic analysis of cracks on bimaterial interfaces: Part I – small scale yielding. J Appl Mech 1988;55:299–316.
[6] Zhang ZL, Hauge M, Thaulow C. Two-parameter characterization of near-tip fields of a bi-material elastic–plastic interface crack. Int J Fract 1996;79:65–83.

[7] Ganti S, Parks DM, McClintock FA. Analysis of strength mis-matched interface cracks in SSY. In: Schwalbe K-H, Kocak M, editors. Mis-matching of interfaces and welds. Geestacht: GKSS Research Center Publications; 1997. p. 3–16.
[8] Kim Y-Y, Lin G, Cornec A, Schwalbe K-H. Effect of elastic and plastic mismatching on interfacial crack-tip fields in contained yielding. In: Schwalbe K-H, Kocak M, editors. Mis-matching of interfaces and welds. Geesthacht: GKSS Research Center Publications; 1997. p. 135–48.
[9] Thaulow C, Hauge M, Zhang ZL, Ranestad Ø, Fattorini F. On the interrelationship between fracture toughness and material mismatch for cracks located at the fusion line of weldments. Engng Fract Mech 1999;64:367–82.
[10] Drugan WJ, Rice JR, Sham T-L. Asymptotic analysis of growing plane strain cracks in elastic-ideally plastic solids. J Mech Phys Solids 1982;30:447–73.
[11] Dean RH, Hutchinson JW. Quasi-static steady crack growth in small-scale yielding. Fracture mechanics: twelfth conference. ASTM STP 700. American Society for Testing and Materials; 1980. p. 383–405.
[12] Parks DM, Lam PS, McMeeking RM. Some effects of inelastic constitutive models on crack tip fields in steady quasistatic growth. In: Advances in Fracture Research, 5th International Conference on Fracture, Cannes; 1981. p. 2607–14.
[13] Varias AG, Shih CF. Quasi-static crack advance under a range of constraints – steady-state fields based on a characteristic length. J Mech Phys Solids 1993;41:835–61.
[14] O'Dowd NP, Shih CF, Dodds Jr RH. The role of geometry and crack growth on constraint and implications for ductile/brittle fracture. In: Mark Kirk, Ad Bakker, editors. Constraint effects in fracture. Theory and applications. ASTM STP 1244, vol. 2. Philadelphia: American Society for Testing and Materials; 1995. p. 134–59.
[15] Xia L, Shih CF. Ductile crack growth – II. Void nucleation and geometry effects on macroscopic fracture behaviour. J Mech Phys Solids 1995;43:1953–81.
[16] Ruggieri C, Dodds Jr RH. A transferability model for brittle fracture including constraint and ductile tearing effects: a probabilistic approach. Int J Fract 1996;79:309–40.
[17] Trädegård A, Nilsson F, Östlund S. J-Q characterization of propagating cracks. Int J Fract 1998;94:357–69.
[18] Østby E, Thaulow C, Zhang ZL. Numerical simulations of specimen size and mismatch effects in ductile crack growth – Part I: Tearing resistance and crack growth paths. Engng Fract Mech 2006, in press, doi:10.1016/j.engfracmech.2006.09.013.
[19] Gurson AL. Plastic flow and fracture of ductile materials incorporating void nucleation, growth and coalescence, PhD thesis, Brown University; 1975.
[20] Tvergaard V. Influence of voids on shear band instability under plane strain conditions. Int J Fract 1981;17:389–407.
[21] Tvergaard V. On localization in ductile materials containing spherical voids. Int J Fract 1982;18:237–52.
[22] Zhang ZL, Thaulow C, Ødegård J. A complete Gurson model approach for ductile fracture. Engng Fract Mech 2000;67:155–68.
[23] Xia L, Shih CF. Ductile crack growth – I. A numerical study using computational cells with microstructurally-based length scales. J Mech Phys Solids 1995;43:233–59.
[24] Hancock JW, Reuter WG, Parks DM. Constraint and toughness parameterized by T. In: Hackett EM, Schwalbe K-H, Dodds RH, editors. ASTM STP 1171. Constraint effects in fracture. Philadelphia: American Society for Testing and Materials; 1993. p. 21–40.
[25] Xia L, Shih CF, Hutchinson JW. A computational approach to ductile crack growth under large scale yielding conditions. J Mech Phys Solids 1995;43:389–413.
[26] Østby E, Zhang ZL, Thaulow C. Constraint effect on the near tip stress fields due to difference in plastic work hardening for bi-materials interface cracks in small scale yielding. Int J Fract 2001;111:87–103.
[27] Moran PM, Shih CF. Crack growth and cleavage in mismatched welds: a micromechanics study using a cell model. Int J Fract 1998;92:153–74.
[28] Burstow MC, Howard IC. Damage mechanics models of ductile crack growth in welded specimens. Fatigue Fract Engng Mater Struct 2000;23:691–708.
[29] Hao S, Brocks W, Kocak M, Schwalbe K-H. On interface crack growth and the criterion to determine the direction of ductile crack propagation. In: Karihaloo BL, Mai, Y-W, Ripley MI, Ritchie RO, editors. Advances in fracture research, ninth international conference on fracture, Sydney; 1997. pp. 2627–34.
[30] Thaulow C, Zhang ZL, Ranestad Ø, Hauge M. J-Q-M. Approach for failure assessment of fusion line cracks: two materials and three materials models, In: Paris PC, Jerina KL, editors. Fatigue and fracture mechanics vol. 30th, ASTM STP 1360, America Society for Testing and Materials, West Conshohcken; 2000. pp. 102–14.
[31] McClintock FA. Plasticity aspects of fracture. In: Liebowitz H, editor. Fracture, vol . 3. New York: Academic Press; 1971. p. 47–225.
[32] Beremin FH. A local criterion for cleavage fracture of a nuclear pressure vessel steel. Met Trans A 1983;14A:2277–87.
[33] Xia L, Shih CF. Ductile crack growth – III. Transition to cleavage fracture incorporating statistics. J Mech Phys Solids 1996;44:603–39.
[34] Thaulow C, Østby E, Nyhus B, Zhang ZL, Skallerud B. Constraint correction of high strength steel. Selection of test specimens and application of direct calculations. Engng Fract Mech 2004;71:2417–33.